ACS Macro Letters

Letter

pubs.acs.org/macroletters

Influence of the Acceptor Composition on Physical Properties and Solar Cell Performance in Semi-Random Two-Acceptor Copolymers

Beate Burkhart, Petr P. Khlyabich, and Barry C. Thompson*

Department of Chemistry, Loker Hydrocarbon Research Institute, and Center for Energy Nanoscience, University of Southern California, Los Angeles, California 90089-1661, United States

Supporting Information

ABSTRACT: Five novel semi-random poly(3-hexylthiophene) (P3HT) based donor−acceptor copolymers containing either thienopyrroledione (TPD) or both diketopyrrolopyrrole (DPP) and TPD acceptors were synthesized by Stille copolymerization, and their optical, electrochemical, charge transport, and photovoltaic properties were investigated. Poly(3-hexylthiophene-thiophene-thienopyrroledione) polymers P3HTT-TPD-10% and P3HTT-TPD-15% with either 10% or 15% acceptor content were synthesized as a point of reference. Two-acceptor polymers containing both TPD and DPP were synthesized with varying acceptor ratios to fine-tune electrooptical properties, namely, P3HTT-TPD-DPP (1:1) (7.5% TPD and 7.5% DPP), P3HTT-TPD-DPP (2:1) (10% TPD and 5% DPP), and P3HTT-TPD-DPP (1:2) (5% TPD and 10% DPP). The two-acceptor copolymers have broad and uniformly strong absorption profiles from 350−850 nm with absorption coefficients up to 8 × 10^4 cm^{-1} at ∼700 nm for P3HTT-TPD-DPP (1:2). This is reflected in the photocurrent responses of polymer:fullerene bulk heterojunction solar cells with $PC_{61}BM$ as an acceptor where P3HTT-TPD-DPP (1:1) and P3HTT-TPD-DPP (1:2) have peak external quantum efficiency (EQE) values of 61% and 68% at 680 nm, respectively, and at 800 nm show impressive EQE values of 29% and 40%. Power conversion efficiencies in solar cells of P3HTT-TPD-10% and P3HTT-TPD-15% are moderate (2.08% and 2.22%, respectively), whereas two-acceptor copolymers achieve high efficiencies between 3.94% and 4.93%. The higher efficiencies are due to a combination of very large short-circuit current densities exceeding 16 mA/cm^2 for P3HTT-TPD-DPP (1:2), which are among the highest published values for polymer solar cells and are considerably higher than those of previously published two-acceptor polymers, as well as fill factors over 0.60. These results indicate that semi-random copolymers containing multiple distinct acceptor monomers are a very promising class of polymers able to achieve large current densities and high efficiencies due to favorable properties such as semicrystallinity, high hole mobility, and importantly broad, uniform, and strong absorption of the solar spectrum.

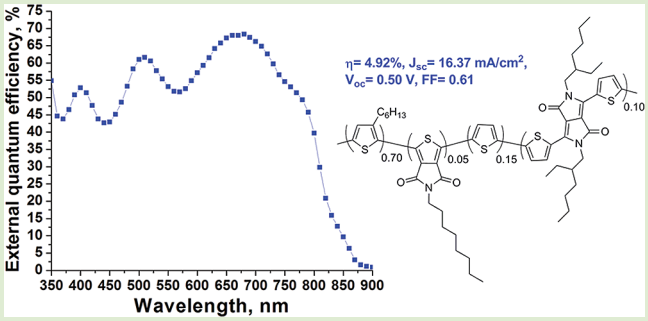

Polymer bulk heterojunction (BHJ) solar cells offer many interesting properties such as flexibility, being lightweight, and low cost that potentially enable a widespread commercial application.[1] Tremendous research effort over the past decade has led to an efficiency increase from below 3% to over 8% in the academic literature with companies such as Polyera reporting 9% for polymer:fullerene BHJs of unknown polymer structure.[2−9] In spite of this impressive increase, new and innovative approaches are still necessary to obtain solar cells with efficiencies in the range of 10−15%, which are envisioned to compete with inorganic solar cells.[10,11] The efficiency of a polymer solar cell is proportional to the short-circuit current density (J_{sc}), the open-circuit voltage (V_{oc}), and the fill factor (FF) requiring these values to be optimized to reach maximum efficiencies. Of great importance is the J_{sc}, where poor spectral coverage by organics is a significant limitation relative to silicon-based solar cells. The J_{sc} is related to the product of the breadth and intensity with which polymers absorb the solar spectrum, where the broader and more intense the absorption the larger J_{sc} can theoretically be.[12] The general approach to increasing the J_{sc} has been to focus on low band gap polymers capable of extending the absorption range into the red and near-infrared (NIR). Typically, perfectly alternating copolymers of electron-rich and electron-poor units are used to target these optical properties via the so-called donor−acceptor approach (D/A). Interestingly in most cases polymers with lower band gaps achieved by the D/A approach do not show broadened absorption, but instead the absorption maxima is shifted toward the NIR, thereby decreasing the number of photons the polymer absorbs in the visible region of the solar spectrum and ultimately limiting the achievable photocurrent.[13−17]

Recently we reported a class of D/A copolymers called semi-random polymers mainly consisting of rr-P3HT with small amounts (between 5 and 17.5%) of acceptor monomer randomly distributed in the backbone.[18−20] The randomized

Received: April 22, 2012
Accepted: May 8, 2012
Published: May 11, 2012

   dx.doi.org/10.1021/mz300197c | *ACS Macro Lett.* 2012, 1, 660−666

Scheme 1. Synthesis of (a) TPD Containing Semi-random Polymers P3HTT-TPD-10% and P3HTT-TPD-15% and (b) Two-Acceptor Polymers Containing TPD and DPP (P3HTT-TPD-DPP (1:1), P3HTT-TPD-DPP (2:1), and P3HTT-TPD-DPP (1:2))

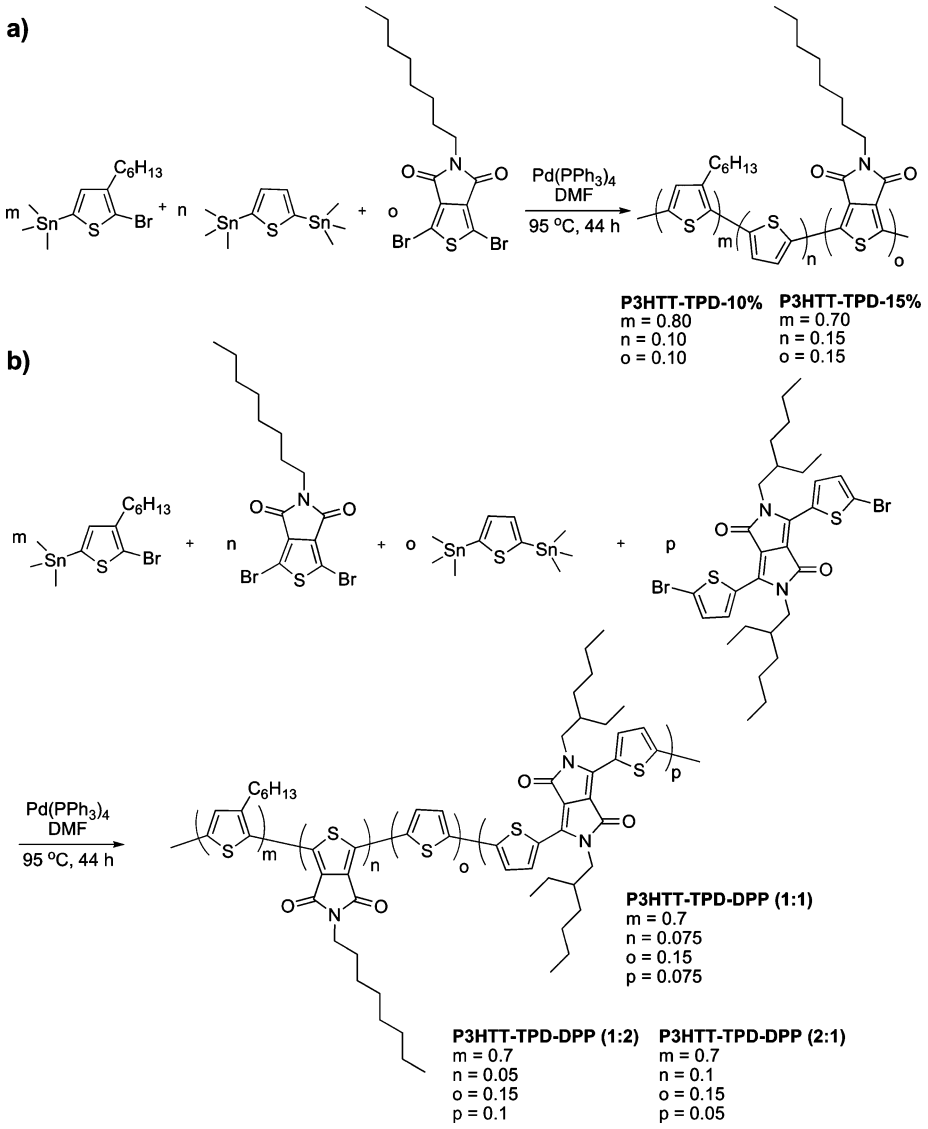

sequence distribution of monomers generates broadly absorbing, multichromophoric polymers which retain a certain degree of structural order due to restricted monomer linkage patterns. Not only do the resulting polymers show very broad and intense absorption profiles, but they also retain many attractive properties of rr-P3HT such as semicrystallinity, high hole mobility, and optimal blending with fullerenes at favorable ratios. Additionally, semi-random polymers have shown high efficiencies of up to 5% in solar cells with $PC_{61}BM$.[19] This is in contrast to reported random D/A copolymers, which, despite broadened absorption, often suffer from low hole mobilities due to a disordered polymer structure as well as the necessity of unfavorable polymer:fullerene ratios with high fullerene loadings.[21−23]

Of special interest among the semi-random polymers is P3HTT-TP-BTD containing two distinct acceptors, benzothiadiazole (BTD) and thienopyrazine (TP), with a total acceptor content of 17.5%.[20] This polymer displayed unprecedented strong and uniform light absorption properties with an absorption onset at 1000 nm and a peak absorption coefficient at 750 nm of almost 9×10^4 cm^{-1}. Despite this, the solar cell efficiency was very low at only 0.43%. For comparison, other random conjugated copolymers containing multiple distinct acceptors in the polymer backbone have received very little attention for application as donors in solar cells with only a few examples reporting solar cell data.[24−27] Such polymers generally show broad absorption of the solar spectrum, and solar cell efficiencies of up to 3.7% with $PC_{71}BM$ have been reported.[25] Even though the photocurrent in the latter case could be primarily attributed to absorption by $PC_{71}BM$, the achieved efficiency highlights the unexploited potential of using multiple acceptors in D/A copolymers.

Here we report the first examples of semi-random copolymers containing multiple distinct acceptor monomers that show high efficiencies in polymer:$PC_{61}BM$ solar cells, which is primarily attributed to broad and intense absorption of the solar spectrum into the near-infrared (NIR) region. We have chosen diketopyrrolopyrrole (DPP) and thienopyrroledione (TPD) as the acceptor units, and the effect of varying the ratio between acceptor monomers (while keeping the overall

dx.doi.org/10.1021/mz300197c | ACS Macro Lett. 2012, 1, 660−666

acceptor content constant at 15%) on polymer properties as well as solar cell performance is described. For this study five novel semi-random D/A copolymers were synthesized, characterized, and tested in BHJ solar cells with $PC_{61}BM$, where broad absorption in the two-acceptor polymers led to short-circuit current densities exceeding 16 mA/cm^2 and efficiencies reaching 5%.

The synthesis of all five new polymers was carried out using a previously established protocol for semi-random copolymers.[20] P3HTT-TPD-10% and P3HTT-TPD-15% (P3HTT-TPD stands for poly(3-hexylthiophene-thiophene-thienopyrroledione) and the number indicates the acceptor content in percent) were synthesized by copolymerizing 2-bromo-5-trimethyltin-3-hexylthiophene with 2,5-bis(trimethyltin)-thiopene and either 10 or 15% of dibromo-thienopyrroledione in DMF at 95 °C with $Pd(PPh_3)_4$ as the catalyst (Scheme 1a). Two-acceptor copolymers were made in an identical manner (Scheme 1b) with the addition of dibromo-bisthiophene-diketopyrrolopyrrole and varying the ratio of acceptors for a total acceptor content of 15% resulting in P3HTT-TPD-DPP (1:1) (7.5% TPD and 7.5% DPP), P3HTT-TPD-DPP (2:1) (10% TPD and 5% DPP), and P3HTT-TPD-DPP (1:2) (5% TPD and 10% DPP). The total acceptor monomer content was chosen as 15% to ensure good solubility of the resulting two-acceptor copolymers as well as to retain their P3HT-like character while providing a broad enough range over which to vary the relative content of the two acceptor monomers. As with our previously published examples of semi-random polymers, the two-acceptor polymers benefit from a highly reproducible synthesis and batch-to-batch consistency of polymer properties.[18−20]

Molecular weights determined by gel permeation chromatography (GPC; calibrated with polystyrene standards) after Soxhlet purification are between 11 730 and 22 630 g/mol (see Synthetic Procedures in the Supporting Information, SI) with the differences mainly due to decreased solubility of some of the polymers. Polymer structures, and especially acceptor contents, were confirmed using ^{1}H NMR by comparing the integration of distinct acceptor peaks (both in the aromatic and alkyl region) with the benzylic CH_2 peaks of 3-hexylthiophene at ∼2.7 ppm (SI, Figures S1−S5). Importantly monomer content and especially acceptor ratios in the polymers match the monomer feed ratio. DPP was chosen as one of the acceptors as it minimizes steric hindrance and induces planarity, thus enhancing the crystallinity of the polymers.[28−30] Semi-random copolymers containing DPP have previously shown high solar cell efficiencies.[19] TPD on the other hand has recently gained significant attention and has been used in many D/A copolymers with high solar cell efficiencies generally showing large V_{oc} and strong absorption in the visible region of the solar spectrum.[17,31−35] As the previously studied P3HTT-DPP-15% (with the same acceptor content as the investigated two-acceptor polymers) suffers from moderate V_{oc} (0.51 eV) and also unbalanced absorption that is weaker in the visible region, TPD was chosen as the complementary acceptor to increase both the V_{oc} and absorption intensity at shorter wavelengths.

The optical properties of all synthesized semi-random copolymers in *o*-dichlorobenzene (*o*-DCB) solutions (see SI, Figure S6) and thin film (Figure 1) were studied using UV−vis spectroscopy. P3HTT-TPD-10% and P3HTT-TPD-15% show a slight broadening of the absorption (Figure 1a) compared to P3HT and only one absorption peak with absorption onsets of

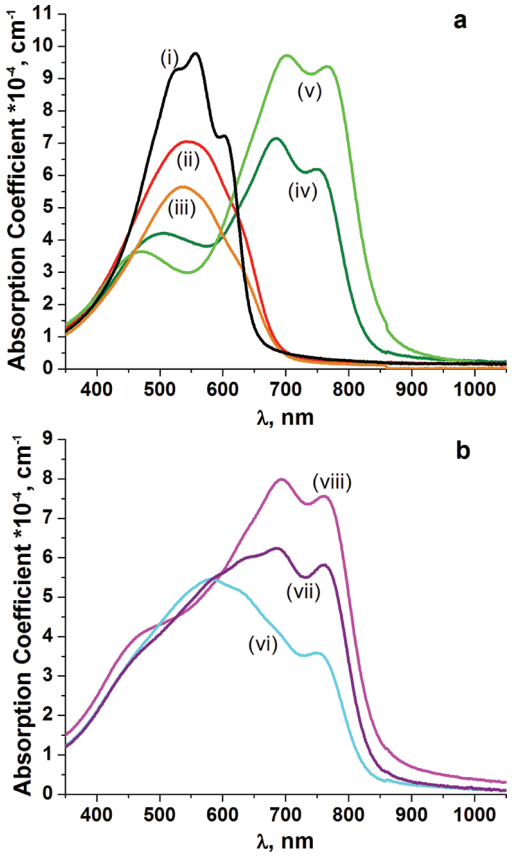

Figure 1. UV−vis absorption spectra of polymers in thin films (spin-coated from *o*-DCB and solvent annealed for 20 min under N_2) for (a) polymers containing one acceptor (either TPD or DPP) and P3HT synthesized by the same method for reference and (b) polymers containing two acceptors (TPD and DPP). (i) P3HT (black line), (ii) P3HTT-TPD-10% (red line), (iii) P3HTT-TPD-15% (orange line), (iv) P3HTT-DPP-10% (dark green line), (v) P3HTT-DPP-15% (light green line), (vi) P3HTT-TPD-DPP (2:1) (cyan line), (vii) P3HTT-TPD-DPP (1:1) (purple line), and (viii) P3HTT-TPD-DPP (1:2) (magenta line).

680 nm and 690 nm, respectively. P3HTT-DPP-10% and P3HTT-DPP-15% have been published previously[19] and exhibit a significantly decreased optical band gap relative to P3HT with a broad absorption profile showing two distinct absorption bands which can be attributed to the $\pi-\pi^*$ band and the intramolecular charge transfer (ICT) band. Figure 1a illustrates that semi-random copolymers containing either TPD or DPP have complementary absorption profiles which would allow for strong and uniform absorption of the solar spectrum if combined. The absorption profiles of the copolymers containing both TPD and DPP are shown in Figure 1b with all three polymers absorbing the solar spectrum very broadly into the NIR and with high peak absorption coefficients reaching 8 × 10^4 cm^{-1} at ∼700 nm for P3HTT-TPD-DPP (1:2). P3HTT-TPD-DPP (1:1) has an absorption onset at 836 nm, corresponding to an optical band gap of 1.48 eV, with a uniform absorption profile enveloping the absorption profiles of both P3HTT-TPD-10% and P3HTT-DPP-10%. Increasing the TPD content to 10% gives P3HTT-TPD-DPP (2:1), which shows a distinct absorption peak at 583 nm, slightly red-shifted from the absorption peak of P3HTT-TPD-10% and P3HTT-TPD-15% around 540 nm, whereas the long wavelength absorption coefficient is considerably reduced compared to

dx.doi.org/10.1021/mz300197c | *ACS Macro Lett.* 2012, 1, 660−666

Table 1. Electronic and Photovoltaic Properties of P3HTT-TPD-10%, P3HTT-TPD-15%, P3HTT-TPD-DPP (1:1), P3HTT-TPD-DPP (2:1), and P3HTT-TPD-DPP (1:2) as well as Optimized Solar Cell Results of P3HT, P3HTT-DPP-10%, and P3HTT-DPP-15% with $PC_{61}BM$ as an Acceptor

polymer:$PC_{61}BM$ (ratio)	HOMO[a] (eV)	E_g[b] (optical) (eV)	SCLC hole mobility[c] ($cm^2/(Vs)$)	J_{sc}[d] (mA/cm^2)	V_{oc} (V)	FF	η_{avg} (η_{peak}) (%)
P3HT[e] (1:0.9)	5.20	1.90	2.6×10^{-4}	9.87	0.60	0.64	3.79 (3.90)
P3HTT-TPD-10%[g] (1:1.5)	5.40	1.82	0.8×10^{-4}	5.38	0.72	0.58	2.22 (2.30)
P3HTT-TPD-15%[g] 1:1.3)	5.40	1.80	0.7×10^{-4}	5.33	0.68	0.56	2.02 (2.08)
P3HTT-DPP-10%[e] (1:1.3)	5.20	1.51	2.3×10^{-4}	14.62	0.59	0.64	5.53 (5.73)
P3HTT-DPP-15%[e] (1:2.6)	5.20	1.46	1.3×10^{-4}	14.28	0.51	0.65	4.66 (4.72)
P3HTT-TPD-DPP (1:1)[f] (1:1.7)	5.35	1.48	1.5×10^{-4}	15.26	0.51	0.64	4.93 (5.03)
P3HTT-TPD-DPP (2:1)[f] (1:1.5)	5.30	1.50	1.6×10^{-4}	11.67	0.55	0.62	3.94 (4.11)
P3HTT-TPD-DPP (1:2)[f] (1:2.0)	5.20	1.47	1.9×10^{-4}	16.37	0.50	0.61	4.92 (4.97)

[a]Cyclic voltammetry (vs Fc/Fc^+) in acetonitrile containing 0.1 M $TBAPF_6$. [b]Optical band gaps from onset of absorption in UV−vis spectra of solvent-annealed films. [c]Measured for neat polymer films. [d]Mismatch corrected. [e]Spin-coated from *o*-DCB and placed in the N_2 cabinet before aluminum deposition for 30 min. [f]Spin-coated from *o*-DCB and placed in the N_2 cabinet before aluminum deposition for 20 min. [g]Spin-coated from chlorobenzene (CB) and tested as-cast.

P3HTT-TPD-DPP (1:1). The absorption onset is blue-shifted compared to P3HTT-TPD-DPP (1:1) with an optical band gap of 1.50 eV, which is likely due to the increased amount of TPD acceptor, considering that P3HTT-TPD-10% has a larger band gap than P3HTT-DPP-10%. On the other hand, P3HTT-TPD-DPP (1:2), which contains twice as much DPP (10%) as TPD (5%), has a distinct absorption peak at 693 nm corresponding to the ICT band of P3HTT-DPP-10% and P3HTT-DPP-15%, together with a vibronic shoulder at 761 nm. P3HTT-TPD-DPP (1:2) also has the lowest optical band gap (1.47 eV), with an absorption onset at 846 nm. The vibronic shoulder visible in both P3HTT-DPP-10% and P3HTT-DPP-15% is retained in all three of the two-acceptor polymers, suggesting that the semicrystalline nature of these polymers is preserved. This is further supported by the fact that all polymers show a red-shift going from *o*-DCB solution (SI, Figure S6) to thin film, indicating increased order in the solid state. Overall, adding a second acceptor gives polymers with intense and broad absorption profiles mimicking the weighted sum of the corresponding one-acceptor polymer absorption profiles with absorption peaks rising or falling according to the change in ratio of acceptors.

To verify the formation of semicrystalline polymer films, grazing-incidence X-ray diffraction (GIXRD) was used (see SI, Figures S8 and S9). P3HTT-TPD-10% and P3HTT-TPD-DPP (2:1) are both amorphous when solvent annealed but semicrystalline when thermally annealed at 145 °C for 45 min with an interchain distance (100) of 17.00 Å and 16.36 Å, respectively. Both P3HTT-TPD-DPP (1:1) and P3HTT-TPD-DPP (1:2) are already semicrystalline when solvent annealed with interchain distances of 16.50 Å and 15.96 Å (SI, Figure S9). This distance decreases slightly for P3HTT-TPD-DPP (1:1) after thermal annealing (from 16.50 to 16.08 Å), whereas it remains the same for P3HTT-TPD-DPP (1:2), although the intensity of the diffraction peak for P3HTT-TPD-DPP (1:2) increases considerably upon annealing. P3HTT-TPD-15% on the other hand is completely amorphous even after thermal annealing, and it is also observed that increasing amounts of TPD in the two-acceptor polymers reduces the intensity of the diffraction peaks, indicating that in semi-random copolymers TPD hinders order in the solid state (see SI, Figures S8 and S9). The interchain distances of the two-acceptor copolymers are comparable to P3HTT-DPP-15% (16.2 Å after annealing) but are considerably larger than that of P3HTT-DPP-10% (14.7 Å as cast and 15.3 Å after annealing). This is likely due to a combination of the increased amount of longer and branched alkyl side-chains compared to P3HTT-DPP-10% as well as the introduction of TPD which gives a larger (100) interchain distance (17.00 Å) in P3HTT-TPD-10%.

The highest occupied molecular orbital (HOMO) levels of all polymers in thin film were measured by cyclic voltammetry with ferrocene as a reference (Fc/Fc^+ = 5.1 eV),[36,37] and the values are summarized in Table 1. P3HTT-TPD-10% and P3HTT-TPD-15% show a HOMO of 5.40 eV which is considerably lower than that of both P3HTT-DPP-10% and P3HTT-DPP-15% (measured previously as 5.20 eV)[19] and consistent with literature values for TPD-containing perfectly alternating D/A copolymers.[32−35] Interestingly this is consistent with our previous findings that the type of acceptor monomer rather than the amount influences the HOMO energy of semi-random copolymers.[19,20] As expected P3HTT-TPD-DPP (1:1) and P3HTT-TPD-DPP (2:1) have intermediate HOMO levels with values of 5.35 eV and 5.30 eV, respectively. P3HTT-TPD-DPP (1:2) on the other hand has the same HOMO level as P3HTT-DPP-10% and P3HTT-DPP-15% at 5.20 eV suggesting that DPP has a stronger influence on the HOMO energy level than TPD.

Hole mobilities for neat polymers determined with the space-charge limited current (SCLC) method are all on the same order of magnitude as P3HT, which was measured as 2.6×10^{-4} $cm^2/(Vs)$ (see Table 1). It is observed that polymers containing DPP as an acceptor (either by itself or in combination with TPD) have a higher mobility than polymers containing only TPD (for example, P3HTT-TPD-DPP (2:1) has a mobility of 1.6×10^{-4} $cm^2/(Vs)$ and P3HTT-TPD-15% has a mobility of 0.7×10^{-4} $cm^2/(Vs)$). This is generally consistent with the results from the GIXRD measurements and the observed trend that the degree of crystallinity goes down with increasing amounts of TPD. An interesting case is P3HTT-TPD-10% which has a lower mobility than P3HTT-TPD-DPP (2:1) even though both polymers have the same TPD content and a qualitatively similar level of crystallinity when thermally annealed. One possible explanation for this is that the DPP unit facilitates $\pi-\pi$-stacking in the solid state (which we are not able to observe with our diffractometer) thus improving charge transport.[29,38]

Considering the broad and intense absorption into the NIR, semicrystalline nature, high hole mobilities, and lower-lying HOMO levels compared to P3HTT-DPP-10% and P3HTT-DPP-15%, the investigated two-acceptor polymers are promis-

dx.doi.org/10.1021/mz300197c | *ACS Macro Lett.* 2012, 1, 660−666

ing candidates as donors in combination with a fullerene acceptor in organic BHJ solar cells. BHJ solar cells in a conventional device configuration of ITO/PEDOT:PSS/polymer:$PC_{61}BM$/Al were fabricated in air (see the SI for detailed solar cell fabrication procedures). The optimized polymer:$PC_{61}BM$ weight ratios are shown in Table 1 and range between 1:1.5 and 1:2.0 for two-acceptor polymers. Interestingly, these ratios are intermediate relative to the limiting cases of one-acceptor polymers P3HTT-TPD-15% (1:1.3) and P3HTT-DPP-15% (1:2.6), which have the same overall acceptor monomer content. Optimal processing conditions include slow solvent evaporation (solvent annealing) from the polymer:$PC_{61}BM$ blends after spin-coating and prior to aluminum deposition for P3HT, two-acceptor, and DPP-containing polymers. The active layer thickness for all solar cells is between 75 nm and 85 nm. Table 1 lists η, V_{oc}, FF, and mismatch corrected[39] J_{sc} obtained under simulated AM 1.5G illumination (100 mW/cm^2) ($J-V$ curves are shown in the SI, Figure S10). P3HT:$PC_{61}BM$ solar cells were fabricated as a point of reference, and an average efficiency of 3.79% was measured with a peak efficiency of 3.90%, which is slightly lower than literature champion values.[40] This difference is primarily attributed to solar cell fabrication and measurement in air as opposed to a protected environment in a glovebox. Fill factors (FF) of all solar cells are extremely high, in the range of 0.56 to 0.65, indicating that the devices work extremely well due to balanced charge-carrier mobilities and optimized morphologies.[41,42] P3HTT-TPD-10% and P3HTT-TPD-15% show moderate solar cell performances of 2.22% and 2.02% attributed to their relatively narrow and weak absorption profiles, which are reflected in the moderate J_{sc} values.

As expected from the measured HOMO levels, the V_{oc} of P3HTT-TPD-10% and P3HTT-TPD-15% is increased to 0.72 and 0.68 V compared to 0.59 and 0.51 V for P3HTT-DPP-10% and P3HTT-DPP-15% (Table 1). In both cases the V_{oc} decreases when going from 10 to 15% acceptor content even though this change is not reflected in the measured HOMO levels.[19] Optimized processing conditions have led to a considerable increase in efficiency compared to earlier reported values for both P3HTT-DPP-10% and P3HTT-DPP-15% from 4.94% to 5.53% (average value) and 4.10% to 4.66% (average value), respectively.[19] The measured peak efficiency of P3HTT-DPP-10% of 5.73% is among the highest reported efficiencies for DPP-containing conjugated polymers and, to the best of our knowledge, the highest efficiency ever reported for a DPP-containing polymer when using $PC_{61}BM$ as the acceptor.[28−30,38] Two-acceptor copolymers P3HTT-TPD-DPP (1:1), P3HTT-TPD-DPP (2:1), and P3HTT-TPD-DPP (1:2) show high average efficiencies of 4.93%, 3.94%, and 4.92%, respectively. Contrary to what the HOMO energies indicate, only P3HTT-TPD-DPP (2:1) has an increased V_{oc} compared to P3HTT-DPP-15% (0.55 V vs 0.51 V), whereas both P3HTT-TPD-DPP (1:1) and P3HTT-TPD-DPP (1:2) have V_{oc} values which are lower at 0.51 V and 0.50 V, respectively. This seems to indicate that the V_{oc} in these semi-random two-acceptor copolymers is much more determined by DPP than TPD, although the reason for that is still unclear. In agreement with the recorded UV−vis spectra in thin films (Figure 1), both P3HTT-TPD-DPP (1:1) and P3HTT-TPD-DPP (1:2) have very large J_{sc} values of 15.26 mA/cm^2 and 16.37 mA/cm^2, respectively, which are among the highest published values for polymer solar cells[43−45] and considerably higher than J_{sc} values published previously for BHJ solar cells using two-acceptor polymers as the donor.[24,25] P3HTT-TPD-DPP (2:1) has a lower J_{sc} of 11.67 mA/cm^2, mainly due to the reduced absorption at long wavelengths as well as a slightly increased band gap because of the small amount of DPP acceptor in the polymer. The lower J_{sc} is the reason for the lower efficiency of P3HTT-TPD-DPP (2:1) compared to the other two-acceptor polymers even though the FF is comparable and the V_{oc} is slightly higher.

The photocurrent response for all optimized BHJ solar cells is shown in Figure 2. P3HTT-TPD-10% and P3HTT-TPD-15% show a photocurrent response up to 700 nm with moderate peak external quantum efficiencies (EQE) of 40% at 510 nm and 37% at 490 nm, respectively. On the other hand, all two-acceptor polymers as well as the previously reported P3HTT-DPP-10% and P3HTT-DPP-15% show a very strong and uniform photocurrent response all the way from 350 nm out to 850 nm (with the peak at 400 nm due to $PC_{61}BM$ light absorption). P3HTT-TPD-DPP (1:1) and P3HTT-TPD-DPP (1:2) have a peak efficiency of 61% and 68% at 680 nm, respectively, and at 800 nm show EQE values of 29% and 40%, which are rarely achieved at this wavelength with low band gap conjugated polymers. The integrated photocurrents from the EQE measurements match within 5% of those from the mismatch corrected photocurrents measured under simulated AM 1.5G illumination (see SI, Table 1 for mismatch factors).

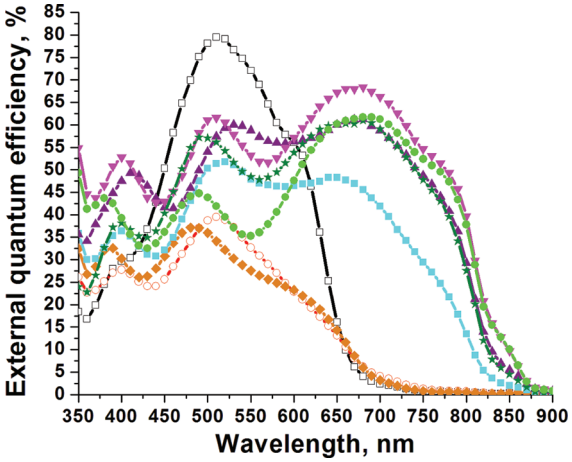

Figure 2. External quantum efficiency of the BHJ solar cells based on P3HT (black open squares), P3HTT-TPD-10% (red open circles), P3HTT-TPD-15% (orange diamonds), P3HTT-DPP-10% (dark green stars), P3HTT-DPP-15% (light green circles), P3HTT-TPD-DPP (1:1) (purple triangles), P3HTT-TPD-DPP (2:1) (cyan squares), and P3HTT-TPD-DPP (1:2) (magenta upside down triangles) with $PC_{61}BM$ as the acceptor, under optimized conditions for device fabrication.

For further characterization the BHJ morphology of the solar cells was analyzed by transmission electron microscopy (TEM), and the recorded images are shown in Figure S11 (SI). All images show uniform, bicontinuous thin films with small length-scales of phase separation between $PC_{61}BM$ and the polymers. The observed morphologies are almost indistinguishable from P3HT:$PC_{61}BM$, which confirms the fact that the newly synthesized polymers retain a similar miscibility with $PC_{61}BM$ and also explains the high observed FF and J_{sc} values.

In summary, we have described a family of five new semi-random copolymers, three of which contain two different acceptor monomers (TPD and DPP) in varying ratios, but at a

dx.doi.org/10.1021/mz300197c | ACS Macro Lett. 2012, 1, 660−666

fixed overall content (15%). The two-acceptor polymers P3HTT-TPD-DPP (1:1), P3HTT-TPD-DPP (2:1), and P3HTT-TPD-DPP (1:2) show very broad and uniform absorption of the solar spectrum with high absorption coefficients. This translates into broad and strong photocurrent responses from 350 nm into the NIR with high EQE values of up to 40% at 800 nm for P3HTT-TPD-DPP (1:2). Efficiencies of close to 5% in BHJ solar cells are observed for two-acceptor semi-random copolymers with currents of over 16 mA/cm^2, rivaling the highest observed values in the literature. This study shows that semi-random copolymers containing multiple distinct acceptor monomers are a very promising class of polymers able to achieve high currents and high efficiencies in solar cells due to broad, uniform, and strong absorption of the solar spectrum. We also highlight that fine-tuning of acceptor monomer ratios is paramount to achieve the best possible efficiencies. Future work will focus on expanding this family of semi-random two-acceptor polymers by investigating other combinations of acceptor monomers, specifically targeting an increase in V_{oc} to achieve polymers combining high J_{sc} and V_{oc} and ultimately higher efficiencies.

■ ASSOCIATED CONTENT

Supporting Information

Synthesis, NMR, UV−vis (solutions), CV, GIXRD, device fabrication procedure, *J*−*V*, and TEM data. This material is available free of charge via the Internet at http://pubs.acs.org.

■ AUTHOR INFORMATION

Corresponding Author

*E-mail: barrycth@usc.edu.

Notes

The authors declare no competing financial interest.

■ ACKNOWLEDGMENTS

This material is based upon work supported as part of the Center for Energy Nanoscience, an Energy Frontier Research Center funded by the U.S. Department of Energy, Office of Science, Office of Basic Energy Sciences, under Award DE-SC0001013. We also thank the Burg Foundation for funding the purchase of the solar simulator used in this work.

■ REFERENCES

(1) Espinosa, N.; Hösel, M.; Angmo, D.; Krebs, F. C. *Energy Environ. Sci.* **2012**, *5*, 5117−5132.
(2) Shaheen, S. E.; Brabec, C. J.; Sariciftci, N. S.; Padinger, F.; Fromherz, T.; Hummelen, J. C. *Appl. Phys. Lett.* **2001**, *78*, 841.
(3) Gendron, D.; Leclerc, M. *Energy Environ. Sci.* **2011**, *4*, 1225−1237.
(4) Thompson, B. C.; Khlyabich, P. P.; Burkhart, B.; Aviles, A. E.; Rudenko, A.; Shultz, G. V.; Ng, C. F.; Mangubat, L. B. *Green* **2011**, 29−54.
(5) Green, M. A.; Emery, K.; Hishikawa, Y.; Warta, W.; Dunlop, E. D. *Prog. Photovolt: Res. Appl.* **2011**, *19*, 565−572.
(6) Chochos, C. L.; Choulis, S. A. *Prog. Polym. Sci.* **2011**, *36*, 1326−1414.
(7) He, Z.; Zhong, C.; Huang, X.; Wong, W.-Y.; Wu, H.; Chen, L.; Su, S.; Cao, Y. *Adv. Mater.* **2011**, *23*, 4636−4643.
(8) Small, C. E.; Chen, S.; Subbiah, J.; Amb, C. M.; Tsang, S.-W.; Lai, T.-H.; Reynolds, J. R.; So, F. *Nature Photon.* **2011**, *6*, 115−120.
(9) Polyera Home Page. http://www.polyera.com/newsflash/polyera-achieves-world-record-organic-solar-cell-performance (accessed April 15, 2012).
(10) He, F.; Yu, L. *J. Phys. Chem. Lett.* **2011**, *2*, 3102−3113.
(11) Son, H. J.; He, F.; Carsten, B.; Yu, L. *J. Mater. Chem.* **2011**, *21*, 18934−18945.
(12) Bundgaard, E.; Krebs, F. *Sol. Energy Mater. Sol. Cells* **2007**, *91*, 954−985.
(13) Allard, N.; Aïch, R. B.; Gendron, D.; Boudreault, P.-L. T.; Tessier, C.; Alem, S.; Tse, S.-C.; Tao, Y.; Leclerc, M. *Macromolecules* **2010**, *43*, 2328−2333.
(14) Najari, A.; Beaupré, S.; Berrouard, P.; Zou, Y.; Pouliot, J.-R.; Lepage-Pérusse, C.; Leclerc, M. *Adv. Funct. Mater.* **2011**, *21*, 718−728.
(15) Wang, E.; Hou, L.; Wang, Z.; Hellström, S.; Zhang, F.; Inganäs, O.; Andersson, M. R. *Adv. Mater.* **2010**, *22*, 5240−5244.
(16) Zhou, H.; Yang, L.; Stuart, A. C.; Price, S. C.; Liu, S.; You, W. *Angew. Chem., Int. Ed.* **2011**, *50*, 2995−2998.
(17) Amb, C. M.; Chen, S.; Graham, K. R.; Subbiah, J.; Small, C. E.; So, F.; Reynolds, J. R. *J. Am. Chem. Soc.* **2011**, *133*, 10062−10065.
(18) Burkhart, B.; Khlyabich, P. P.; Thompson, B. C. *J. Photon. Energy* **2012**, *2*, 021002.
(19) Khlyabich, P. P.; Burkhart, B.; Ng, C. F.; Thompson, B. C. *Macromolecules* **2011**, *44*, 5079−5084.
(20) Burkhart, B.; Khlyabich, P. P.; Cakir Canak, T.; LaJoie, T. W.; Thompson, B. C. *Macromolecules* **2011**, *44*, 1242−1246.
(21) Yu, C.-Y.; Chen, C.-P.; Chan, S.-H.; Hwang, G.-W.; Ting, C. *Chem. Mater.* **2009**, *21*, 3262−3269.
(22) Zhu, Z.; Waller, D.; Gaudiana, R.; Morana, M.; Mühlbacher, D.; Scharber, M.; Brabec, C. *Macromolecules* **2007**, *40*, 1981−1986.
(23) Song, J.; Zhang, C.; Li, C.; Li, W.; Qin, R.; Li, B.; Liu, Z.; Bo, Z. *J. Polym. Sci., Part A: Polym. Chem.* **2010**, *48*, 2571−2578.
(24) Song, J.; Zhang, C.; Li, C.; Li, W.; Qin, R.; Li, B.; Liu, Z.; Bo, Z. *J. Polym. Sci., Part A: Polym. Chem.* **2010**, *48*, 2571−2578.
(25) Tsai, J.-H.; Chueh, C.-C.; Chen, W.-C.; Yu, C.-Y.; Hwang, G.-W.; Ting, C.; Chen, E.-C.; Meng, H.-F. *J. Polym. Sci., Part A: Polym. Chem.* **2010**, *48*, 2351−2360.
(26) Balan, B.; Vijayakumar, C.; Saeki, A.; Koizumi, Y.; Seki, S. *Macromolecules* **2012**, *45*, 2709−2719.
(27) Öktem, G.; Balan, A.; Baran, D.; Toppare, L. *Chem. Commun.* **2011**, *47*, 3933−3935.
(28) Qu, S.; Tian, H. *Chem. Commun.* **2012**, *48*, 3039−3051.
(29) Jung, J. W.; Liu, F.; Russell, T. P.; Jo, W. H. *Energy Environ. Sci.* **2012**, *5*, 6857−6861.
(30) Bijleveld, J. C.; Gevaerts, V. S.; Di Nuzzo, D.; Turbiez, M.; Mathijssen, S. G. J.; de Leeuw, D. M.; Wienk, M. M.; Janssen, R. A. J. *Adv. Mater.* **2010**, *22*, E242−E246.
(31) Zhang, Q. T.; Tour, J. M. *J. Am. Chem. Soc.* **1997**, *119*, 5065−5066.
(32) Zou, Y.; Najari, A.; Berrouard, P.; Beaupré, S.; Réda Aïch, B.; Tao, Y.; Leclerc, M. *J. Am. Chem. Soc.* **2010**, *132*, 5330−5331.
(33) Piliego, C.; Holcombe, T. W.; Douglas, J. D.; Woo, C. H.; Beaujuge, P. M.; Fréchet, J. M. J. *J. Am. Chem. Soc.* **2010**, *132*, 7595−7597.
(34) Chu, T.-Y.; Lu, J.; Beaupré, S.; Zhang, Y.; Pouliot, J.-R.; Wakim, S.; Zhou, J.; Leclerc, M.; Li, Z.; Ding, J.; Tao, Y. *J. Am. Chem. Soc.* **2011**, *133*, 4250−4253.
(35) Najari, A.; Berrouard, P.; Ottone, C.; Boivin, M.; Zou, Y.; Gendron, D.; Caron, W.-O.; Legros, P.; Allen, C. N.; Sadki, S.; Leclerc, M. *Macromolecules* **2012**, *45*, 1833−1838.
(36) Cardona, C. M.; Li, W.; Kaifer, A. E.; Stockdale, D.; Bazan, G. C. *Adv. Mater.* **2011**, *23*, 2367−2371.
(37) Thompson, B. C.; Kim, Y.-G.; McCarley, T. D.; Reynolds, J. R. *J. Am. Chem. Soc.* **2006**, *128*, 12714−12725.
(38) Bronstein, H.; Chen, Z.; Ashraf, R. S.; Zhang, W.; Du, J.; Durrant, J. R.; Shakya Tuladhar, P.; Song, K.; Watkins, S. E.; Geerts, Y.; Wienk, M. M.; Janssen, R. A. J.; Anthopoulos, T.; Sirringhaus, H.; Heeney, M.; McCulloch, I. *J. Am. Chem. Soc.* **2011**, *133*, 3272−3275.
(39) Shrotriya, V.; Li, G.; Yao, Y.; Moriarty, T.; Emery, K.; Yang, Y. *Adv. Funct. Mater.* **2006**, *16*, 2016−2023.
(40) Dang, M. T.; Hirsch, L.; Wantz, G. *Adv. Mater.* **2011**, *23*, 3597−3602.
(41) Kim, M.-S.; Kim, B.-G.; Kim, J. *ACS Appl. Mater. Interfaces* **2009**, *1*, 1264−1269.

(42) Kotlarski, J. D.; Moet, D. J. D.; Blom, P. W. M. *J. Polym. Sci., Part B: Polym. Phys.* **2011**, *49*, 708−711.
(43) Huo, L.; Zhang, S.; Guo, X.; Xu, F.; Li, Y.; Hou, J. *Angew. Chem., Int. Ed.* **2011**, *50*, 9697−9702.
(44) Coffin, R. C.; Peet, J.; Rogers, J.; Bazan, G. C. *Nat. Chem.* **2009**, *1*, 657−661.
(45) Saadeh, H. A.; Lu, L.; He, F.; Bullock, J. E.; Wang, W.; Carsten, B.; Yu, L. *ACS Macro Lett.* **2012**, *1*, 361−365.